



## Polymer Communication

## Shape memory properties of main chain bile acids polymers

Héloïse Thérien-Aubin, Julien E. Gautrot, Yu Shao, Jie Zhang, X.X. Zhu\*

Département de chimie, Université de Montréal, C.P. 6128, Succ. Centre-ville, Montréal, QC H3C 3J7, Canada

## ARTICLE INFO

## Article history:

Received 4 September 2009

Received in revised form

5 November 2009

Accepted 13 November 2009

Available online 17 November 2009

## Keywords:

Bile acid polymers

Shape memory polymers

Wide angle X-ray scattering

## ABSTRACT

Main chain bile acid polymers obtained via entropy-driven ring-opening metathesis are biodegradable polymers with excellent shape memory properties. X-ray scattering was used to study the conformational changes implicated in the shape memory effect of these polymers. Strain induced orientation and ordering was observed upon the drawing of the polymer films. A correlation between ordering and the shape memory performances is observed.

© 2009 Elsevier Ltd. All rights reserved.

## 1. Introduction

Since the commercialization of heat-shrinkable polyethylene in the 1960s, [1] shape memory polymers have attracted tremendous interest [2–8]. In these materials, the original shape is “memorized” either through chemical or physical cross links (such as chain entanglement or micro crystal formation), while the transient shape is maintained by the formation of crystalline domains or only by the glassy state [9–11].

Few monoblock linear uncrosslinked amorphous polymers are able to both memorize the original shape and fix the transient shape. It was shown that polynorbornene derivatives can display high strain fixities and recover their permanent shape when warmed above their glass transition, with relatively low strain recoveries [3,9]. Li et al. described the fast shape recovery of poly(methyl methacrylate) samples embossed above their glass transition, although the deformation applied are small (less than 300  $\mu\text{m}$ ) [9,12]. It is generally accepted that chain entanglement of the high molecular weight polymers is responsible for the recovery of the original shape, whereas the transient shape is fixed by the glassy state.

Recently, we reported the synthesis of a new class of biodegradable shape memory polymers based on bile acids (Fig. 1) [2]. Bile acids are natural molecules present in the human body. They are synthesized in the liver from cholesterol and are ideal building blocks for the design of new polymers for biomedical applications due to their biocompatibility and well controlled chemistry [13].

Shape memory polymers based on bile acids are thermoplastic polymers that can be processed either by solvent casting or by molding. In addition, bile acid-based polyesters did not display any sign of crystallization or covalent cross-links and both their elasticity and shape memory behaviours seem to arise from chain entanglement. In contrast to polynorbornene and poly(methyl methacrylate), they display high strain fixities and recoveries in both warm and cold drawing mode, even after large deformations (above 200% elongation). Here, we investigate further the relationship between shape memory properties and strain-induced molecular ordering in bile acid amorphous polymers.

## 2. Experimental section

## 2.1. Sample preparation

The shape memory polymers based on bile acids were synthesized as reported previously [2,14,15] with details given in the Supporting information. Their characteristics are listed in Table 1. Polymer films were prepared by evaporation of concentrated dichloromethane solutions (100 mg/mL) of the desired polymer in a mould. Rectangular pieces of 0.2 mm  $\times$  4.75 mm  $\times$  2 cm were cut from these films and used for mechanical tests (dimensions of the films were measured with an electronic micrometer ( $\pm 0.001$  mm)).

## 2.2. Thermomechanical analysis

DSC experiments were carried out on a Q2000 calorimeter from TA instruments. The heating/cooling rate was fixed at 10  $^{\circ}\text{C}/\text{min}$ .

\* Corresponding author. Tel.: +1 514 340 5172; fax: +1 514 340 5290.  
E-mail address: [julian.zhu@umontreal.ca](mailto:julian.zhu@umontreal.ca) (X.X. Zhu).

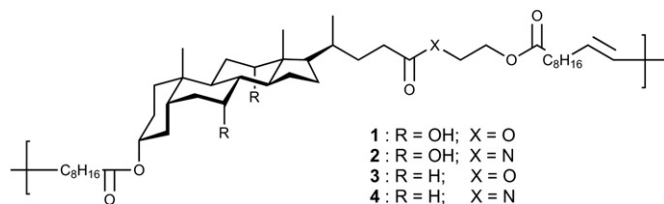


Fig. 1. The chemical structure of the bile acid polymers (1–4).

The  $T_g$  was measured on the second heating run (see Supporting information).

DMA experiments were carried out on a DMA 2980 instrument from TA. Dynamic experiments to measure  $T_g$  were performed at 10 Hz, a preload force of 0.02 N was applied to the sample subject to a heating rate of 1 °C/min and an oscillation amplitude of 10  $\mu$ m. Shape memory experiments were performed in a force-controlled setup. A preload force of 0.01 N was applied to the sample before heating the sample to  $T_g + 10$ . After equilibration for 20 min, the sample was stretched to c.a. 200% of its original length upon the application of a force ramp of 0.5 N/min. The temperature was quickly cooled down to  $T_g - 10$ , and the temperature of the sample was equilibrated for 10 min. Then, the force load was released and the relaxation was measured for 20 min. The temperature was then increased to  $T_g + 10$  and the sample was left to relax for 20 min. At least 2 cycles were performed for each sample. Strain fixity and recovery reported in Table 1 are measured on the second cycle.

### 2.3. X-ray scattering

X-ray scattering studies were carried out on a Bruker D8 Discover diffractometer using a Cu K $\alpha$  radiation source ( $\lambda = 1.542$  Å). The scattering patterns were recorded with a Bruker Hi-Star two-dimensional detector placed at 9.93 cm from the sample. The instrument was calibrated with a standard sample of silver behenate. Temperature was controlled at  $\pm 1$  °C with an Instec STC200 temperature controller. For each diffractogram 1800 scans were accumulated and a scattering background was subtracted from the signal of the sample.

The X-ray diffractograms of stretched samples were recorded at  $T_g - 20$ . The polymer film was stretched at  $T_g + 10$  on the DMA to the desired strain, and then cooled down to room temperature and placed in the X-ray sample holder at the desired temperature. For polymer 4, for which  $T_g$  is below room temperature, the sample was stretched to the desired strain at  $T_g + 10$  and then cooled down to  $-70$  °C and rapidly inserted in the pre-cooled X-ray sample holder.

The errors reported are the standard deviation observed on triplicates.

## 3. Results and discussion

Main chain bile acid polyesters (BAPs) prepared by entropy-driven ring-opening polymerization display excellent shape

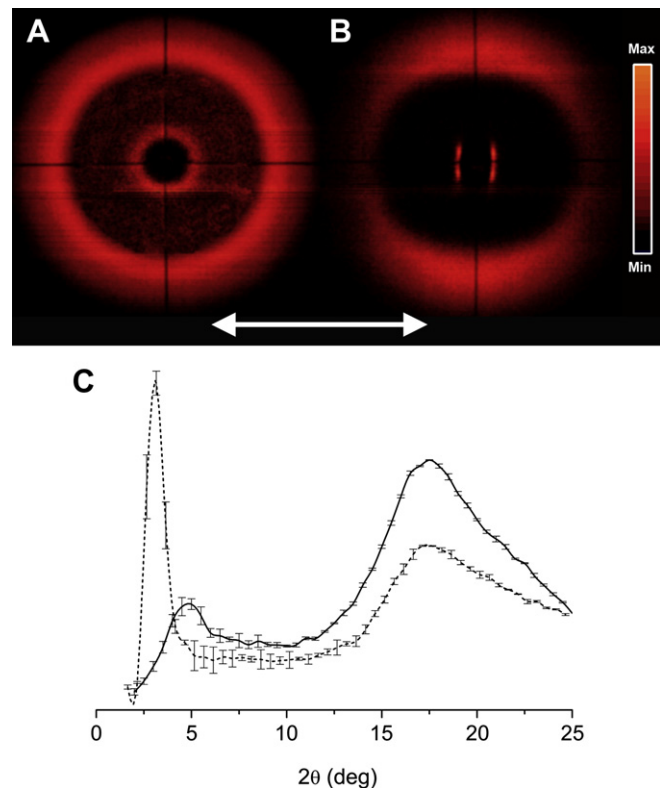


Fig. 2. X-Ray diffractogram of polymer 1, which is typical for the BAPs. (A) Before stretching; (B) After a 400% stretching, and the arrow shows the stretching axis of the polymer film; (C) Integration of the diffractogram in the equatorial direction before (solid line) and after (dashed line) stretching.

memory properties (Table 1) with strain fixity and strain recovery among the best observed for uncross-linked amorphous polymers [2]. BAPs are amorphous as observed by DSC, polarized optical microscopy and wide angle X-ray scattering (WAXS). The WAXS pattern (Fig. 2A) shows two amorphous halos, but the absence of sharp Bragg peak is an evidence of the amorphous state of the polymer both before and after stretching. The absence of crystallinity is further confirmed since no melting was detected by DSC. After stretching, the polymers are still amorphous, but orientation is observed by WAXS (Fig. 2B) as denoted by the arc-shaped halos at  $q = 25$  and  $q = 6.5$  nm $^{-1}$  (corresponding to a diffraction angle of 17.9 and 4.6° and an interplanar distance of c.a. 0.5 and 1.9 nm, respectively). The two halos are perpendicularly oriented to each other.

Few semi-crystalline polymers with bile acid moieties present in the main chains or as side chains have ever been identified, [16,17] while similar steroidal structures (such as cholesterol) when incorporated in polymers do crystallize [18]. This discrepancy is usually ascribed to the bent structure in bile acid, which prevents a close packing needed for the formation of large crystalline

Table 1

Physical characteristics<sup>a</sup> and shape memory properties of the polymers containing bile acids.

Polymer	$M_w$ (kDa)	PDI	$T_g$ (°C)			Strain fixity (%)	Strain recovery (%)
			DMA	DSC	X-Ray		
1	400	1.4	57.4 $\pm$ 0.8	48 $\pm$ 1	40 $\pm$ 3	97.9 $\pm$ 0.7	92 $\pm$ 6
2	120	1.8	88 $\pm$ 3	79 $\pm$ 2	59 $\pm$ 3	95.7 $\pm$ 0.5	99.0 $\pm$ 0.6
3	320	2.2	17 $\pm$ 2	10 $\pm$ 3	13 $\pm$ 4	98.6 $\pm$ 0.5	99.4 $\pm$ 0.5
4	250	1.6	58.6 $\pm$ 0.9	47 $\pm$ 1	38 $\pm$ 4	99.4 $\pm$ 0.3	97 $\pm$ 3

<sup>a</sup> Experimental details of the measurements are described in the Supporting Information.

domains. In this respect, it is not unexpected to observe that polymers 1–4 are totally amorphous. WAXS results show short range order: the first halo corresponding to interchain correlation is observed at ca 5 Å, while the second amorphous halo corresponding to intrachain correlation is observed at ca 19 Å, reflecting the distance between the bile acid repeat units in a polymer chain. These dimensions are in keeping with the relatively large dimension of a bile acid molecule as determined by the crystal structure of the unmodified molecules, [19,20] in comparison to other types of polymers displaying smaller repeat units such as poly(methyl methacrylate) or polystyrene, which typically display spacings between 10 and 14 Å [21]. The interchain spacing increase with temperature (Fig. S2.B) which is consistent with the increase of free volume, while the interplanar distance of 19 Å is temperature independent which is expected for an intrachain correlation. Moreover, the orientation of the two halos after stretching is in keeping with this assignment; the long-range order halo (the distance between two repeating units) becomes oriented along the drawing axis while the second halo (corresponding to the interchain distance) becomes oriented perpendicularly to the drawing axis. A shift in the interchain spacing is observed for the different BAPs. The first halo is 4.95 Å for the polymers made of cholic acid (polymers 1 and 2) but shift to 5.0 Å for the lithocholic acid polymers (polymers 3 and 4) (Fig. S1). This difference may be attributed to the variation of free volume between the BAPs containing cholic acid and lithocholic acid; the presence of the hydroxyl groups on the cholic acid residue may enhance the interactions (through hydrogen bonding) between two polymer chains, thereby reducing the free volume of the polymer. These shifts imply that both the hydroxyl functions of the cholic acid moieties and the presence of an amide bond in the main backbone induce variations in inter-segment spacing.

The WAXS data was used to measure the orientation and ordering when a strain is induced in the samples. The size of the ordered domains is related to the width (FWHM) of the scattering peak through the Scherrer equation, where the size of the ordered domains increase when the peak becomes sharper [22].

$$\tau = \frac{\lambda}{\beta \cos(\theta)} \quad (1)$$

where  $\tau$  is the average apparent size of the ordered domains,  $\lambda$  the wavelength of the X-ray,  $\beta$  the full width at half maximum (FWHM) of the scattering peak,  $\theta$  the position of the scattering peak.

If a cylindrical symmetry is assumed, the orientation distribution function is expressed by a Legendre polynomial of order  $n$ . The second order function, the Hermans orientation function or  $P_2$  function, is given by [23]

$$\langle P_2(\cos \varphi) \rangle = \frac{3\langle \cos^2 \varphi \rangle - 1}{3\cos^2 \sigma - 1} \quad (2)$$

where  $\varphi$  is the azimuthal angle and  $\sigma$  the angle of the drawing direction. The average  $\cos^2 \varphi$  was obtained by the integration of the X-ray diffracted intensity ( $I$ ) for a given  $2\theta$  angle in the azimuthal direction [19].

$$\langle \cos^2 \varphi \rangle = \frac{\int_0^\pi I(\varphi) \cos^2 \varphi \sin \varphi d\varphi}{\int_0^\pi I(\varphi) \sin \varphi d\varphi} \quad (3)$$

A complete alignment parallel to the direction  $\sigma$  will give a  $P_2$  value of +1, while a perpendicular orientation will give  $P_2 = -0.5$ ,

complete randomness gives  $P_2 = 0$ . Here,  $\langle P_2 \rangle$  represents the statistical average of chains axes orientation with respect to the drawing direction.

Upon drawing of the polymer film, the orientation of the polymer chains in the drawing direction increases with respect to the strain applied as observed by the formation of an arc-shape X-ray pattern leading to a preferential azimuthal orientation (Fig. S3). The azimuthal profiles are used to measure the second order orientation function. The  $\langle P_2 \rangle$  of the polymer increases with the applied strain until it reaches a plateau of modest orientation for all four polymers studied (Fig. 3A). The  $\langle P_2 \rangle$  value clearly indicates that the orientation is no longer random. In parallel, the width of the peak in the  $2\theta$  dimension decreases (Fig. S4), which indicates an increase in long-range order (Fig. 3B). The orientation of the polymer chains could favour the establishment of intermolecular interactions leading to the formation of larger ordered domains. While the  $\langle P_2 \rangle$  orientation does not directly correlate with the shape memory properties of the polymer, a strong correlation is observed between strain fixity and the FWHM of the scattering peak (Fig. 4).

The high performance of the main chain bile acid polymer in strain fixity is unexpected for purely amorphous polymer where the transient shape is only fixed by the glassy state of the polymer. Good performance in strain fixity is common in semi-crystalline polymer [1,4,5] where shape recovery occurs upon melting of the crystalline domains. In the case of polymers 1–4 the strain applied to the polymers increases the size of the ordered domains, without leading to the creation of ordered domains large enough to give rise to sharp Bragg diffraction peaks. However, there is a clear relation between the size of the ordered domains (or the FWHM) and the shape memory performance of the polymers (Fig. 4). Ordered domains act as pseudo-cross-linking points helping in freezing the transient shape due to the increased intermolecular interactions. Unstretched samples composed of lithocholic acid (polymers 3 and 4) have smaller ordered domains than the cholic acid polymers (1 and 2). Upon stretching, the polymers containing lithocholic acid become more ordered and show better strain fixity than those containing cholic acid. At high strains, this effect may become less significant as the size of the ordered domains reaches a maximum. At low strains, these domains may be too small to have a large impact on the shape memory properties of the BAPs.

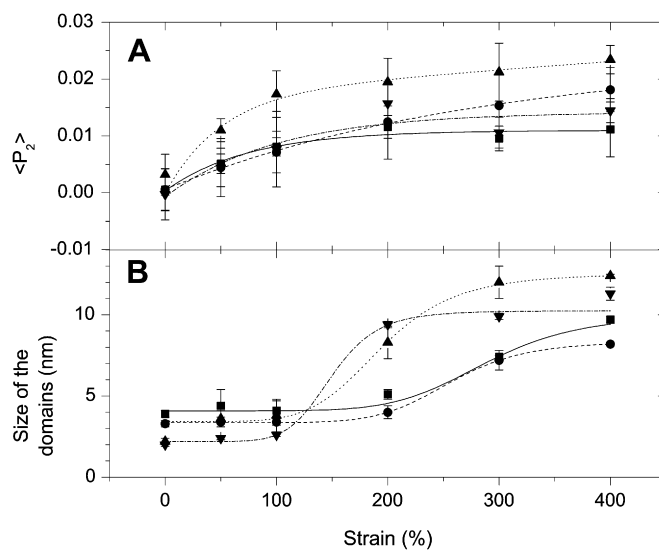
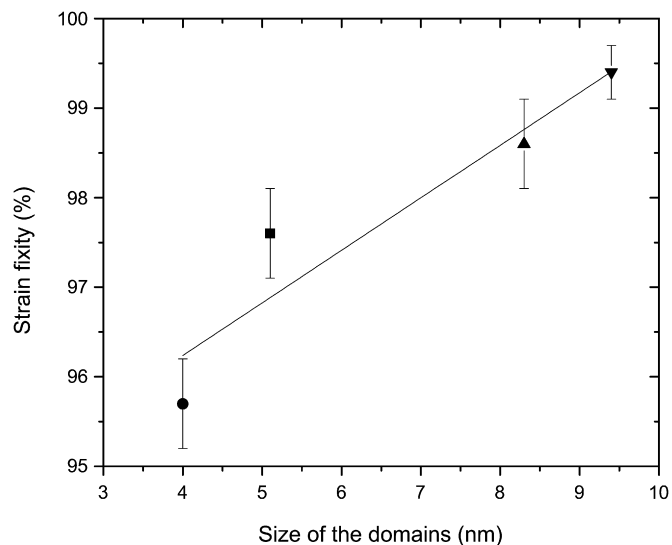


Fig. 3. The variation of (A)  $P_2$  orientation and (B) the size of the ordered domains measured from the FWHM as a function of the strain applied to the polymer film for the scattering peak at ca. 2 nm. Polymers 1 (■), 2 (●), 3 (▲) and 4 (▼). The solid, dotted and dashed lines are guides for the eye.



**Fig. 4.** The relationship between shape memory properties and polymer order when a 200% strain is applied to the polymer films. Polymers 1 (■), 2 (●), 3 (▲) and 4 (▼). The solid line is a guide for the eye.

#### 4. Conclusion

In all the polymers studied, no crystallinity was observed, which is unusual for uncross-linked polymers with shape memory properties. WAXS was used to observe the formation of ordered domains during sample deformation. The shape memory properties of the bile acid polymers result from a combination of the effect of chain entanglement (essential to observe shape memory properties in uncross-linked amorphous polymers) and of the size of the ordered domains (improving strain fixity). The polymers have shown increased orientation and order of the chains upon stretching. Larger ordering in lithocholic acid-containing polymers was observed in comparison to the cholic acid-containing polymers. This may be due to the presence of the extra hydroxyl groups on the cholic acid residues which may hinder the reorganization of the polymer chains in larger ordered domains. Therefore, our results show that, to achieve high shape memory performances in fully amorphous and uncross-linked polymers, it is necessary for the material to display (1) a sharp glass transition associated with

a large drop in storage modulus (2–3 orders of magnitude) and (2) a strain-induced formation of larger ordered domains. These considerations may be the basis of further molecular design that allows manipulation of macromolecular architecture without significantly impairing shape memory properties.

#### Acknowledgments

The authors acknowledge NSERC of Canada, and the Canada Research Chair program for their financial support.

#### Appendix. Supplementary material

Supplementary data associated with this article can be found, in the online version, at doi:10.1016/j.polymer.2009.11.027.

#### References

- [1] Rainer WC, Redding EM, Hitov JJ, Sloan AW, Stewart WD. Heat-shrinkable polyethylene; 1964, US3144398.
- [2] Gautrot JE, Zhu XX. *Macromolecules* 2009;42(19):7324–31.
- [3] Jeon HG, Mather PT, Haddad TS. *Polym Int* 2000;49(5):453–7.
- [4] Ji FL, Zhu Y, Hu JL, Liu Y, Yeung LY, Ye GD. *Smart Mater Struct* 2006;15(6):1547–54.
- [5] Lendlein A, Schmidt AM, Langer R. *Proc Natl Acad Sci U S A* 2001;98(3):842–7.
- [6] Lendlein A, Schmidt AM, Schroeter M, Langer R. *J Polym Sci Pol Chem* 2005;43(7):1369–81.
- [7] Rabani G, Luftmann H, Kraft A. *Polymer* 2006;47(12):4251–60.
- [8] Tobushi H, Hara H, Yamada E, Hayashi S. *Smart Mater Struct* 1996;5(4):483–91.
- [9] Irie M. Shape memory polymers. In: Otsuka K, Wayman CM, editors. *Shape memory materials*. Cambridge University Press; 1998. p. 203–19.
- [10] Lendlein A, Kelch S. *Angew Chem* 2002;41(12):2034–57.
- [11] Liu C, Qin H, Mather PT. *J Mater Chem* 2007;17(16):1543–58.
- [12] Yang F, Li JCM. *J Mater Res* 1997;12(10):2809–14.
- [13] Zhu XX, Nichifor M. *Acc Chem Res* 2002;35(7):539–46.
- [14] Gautrot JE, Zhu XX. *Angewandte chemie. Int Edition* 2006;45(41):6872–4.
- [15] Gautrot JE, Zhu XX. *Chem Commun* 2008;(14):1674–6.
- [16] Gouin S, Zhu XX, Lehnert S. *Macromolecules* 2000;33(15):5379–83.
- [17] Xiao WQ, Zhang BY, Cong YH. *Colloid Polym Sci* 2008;286(3):267–74.
- [18] Zhang JH, Bazuin CG, Freiberg S, Brisse F, Zhu XX. *Polymer* 2005;46(18):7266–72.
- [19] Arora SK, Germain G, Declercq JP. *Acta Cryst Sect B Struct Sci* 1976;B32(2):415–9.
- [20] Campanelli AR, DeSanctis SC, D'Archivio AA, Giglio E, Scaramuzza L. *J Inclusion Phenom Macrocyclic Chem* 1991;11(3):247–56.
- [21] Miller RL, Boyer RF, Heijboer J. *J Polym Sci, Polym Phys* 1984;22(12):2021–41.
- [22] Patterson AL. *Phys Rev* 1939;56(10):978.
- [23] Alexander LE. *X-ray diffraction methods in polymer science*. New York: Wiley-Interscience; 1979.